Femtosecond UV and XUV photoelectron spectroscopy of dissociating methyl iodide

Contact *r.s.minns@soton.ac.uk*

B. Downes-Ward, E. M. Warne, J. Woodhouse, R. S. Minns
Chemistry, University of Southampton, Highfield, Southampton, SO17 1BJ

A. S. Wyatt, P. Majchrzak, G. Karras, Y. Zhang, E. Springate, R. T. Chapman

Central Laser Facility, STFC Rutherford Appleton Laboratory, Didcot, Oxfordshire OX11 0QX

M. A. Parkes

Department of Chemistry, University College London, 20 Gordon Street, London

Introduction

Methyl iodide is a classic system for the study of non-adiabatic processes in photochemical systems [1-3] and stands as a benchmark system for new structural dynamics probes [4,5]. The dynamics of the system can be well described by the potentials in figure 1. Absorption of light around 260 nm leads to population transfer into the Q-band, comprising of the dissociative $^3Q_0$, $^3Q_1$ and $^1Q_1$ states. Absorption across the majority of wavelengths covered by the Q-band is dominated by the $^3Q_0$ state where most of the population is transferred [6]. Once in the excited state the steep gradient along the C-I stretching coordinate leads to rapid dissociation within the first ~100 fs following excitation. En-route to dissociation, there is a crossing between the $^3Q_0$ and $^1Q_1$ states where population can be non-adiabatically transferred between the two states.

At Artemis, we have performed a series of photoelectron spectroscopy experiments using both UV and XUV probe photon energies to monitor the dissociation dynamics following UV excitation at a range of energies across the Q-band. The UV probe measurements utilizes the velocity map imaging (VMI) capabilities to measure both electron kinetic energies and angular distributions at geometries close to the Franck-Condon region, while the XUV measurements used an electron time of flight spectrometer to map the changes in structure over a much broader range of configurations. The experiments demonstrate the extra detail available from time resolved photoelectron spectroscopy measurements when the high resolution UV VMI measurements are combined with the extended geometry range of dynamics covered when using an XUV probe. The detail contained within both provide structural and electronic state measurements that provide detailed information on the initial photodynamics in the Franck-Condon region and structural maps of the extending C-I bond over a much broader range of geometries.

Experiment

The layout of the experiment is broadly similar to that outlined in reference [7]. The output of the amplified femtosecond laser system at Artemis (Red Dragon, KMLabs) generates 30 fs pulses centred around 800 nm, with a pulse energy of approximately 11 mJ. This energy is split before compression to allow for independent tuning of the pump and probe pulse characteristics. The output of compressor one is used to pump a high energy OPA followed by sum frequency generation to generate a few μJ of the tunable UV pump. The probe for the velocity map imaging experiments is produced via second harmonic generation of the 800 nm Red Dragon output, producing approximately 5 μJ of 400 nm light. Absorption of two photons leads to ionization of the excited state population. The XUV probe is generated via high harmonic generation of the second harmonic of the Red Dragon output. Approximately 0.5 mJ of 400 nm light is tightly focused into an argon gas jet generating a series of odd harmonics. The harmonics are passed through a time preserving monochromator [8], separating the 7th harmonic at 22.6 eV and delivering approximately 10^{10} photons per second on target. For all experiments, all beams are reflection focused and overlapped to the interaction point of the spectrometer. For the UV pulses this is a VMI spectrometer of standard Eppink and Parker design as used in ref [9-12]. The XUV experiments have the focus approximately 2 mm before the entrance cone of the electron time-of-flight spectrometer (Kaesdorf ETF11) as used in ref [7]. Spatial overlap of the XUV and UV beams is checked with a LuAG:Ce phosphorescent crystal placed at the interaction region and imaged with a CCD camera. A pure molecular beam of CH_3I is produced via a continuous expansion of the room temperature vapour through a 200 μm hole held a few cm away from the interaction point.

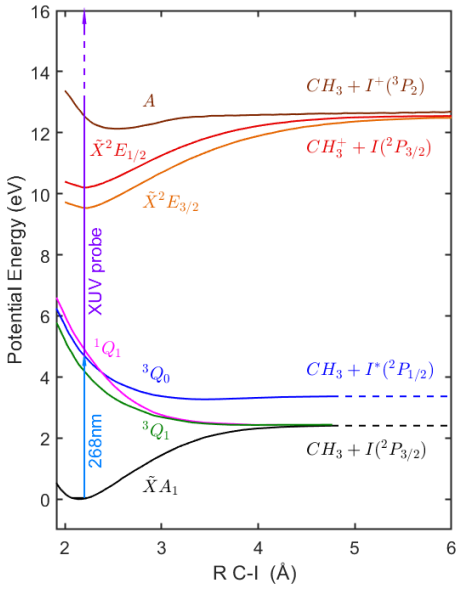

Figure 1. Methyl iodide potential energy surfaces

Results and Discussion

The time-resolved photoelectron spectra obtained from the two types of experiment are summarised in figures 2 and 3. Figure 2 presents the time-resolved spectra obtained with a pump energy around 268 nm corresponding to an energy to the red of the Q-band absorption maximum. At this energy 100% of the excited state population is initially in the $^3Q_0$ state. In figure 2 a, we plot the data from the VMI experiments where we have an effective probe energy of 6 eV from the two photon absorption of the 400 nm probe. Figure 2 b is part of the spectrum obtained from the XUV probe, showing the excited state contribution to the overall signal. At higher binding energies, we also measure the ground state photoelectron spectrum, which shows no time-dependence and is therefore not plotted here. The UV signal following the 268 nm pump shows the most intense features

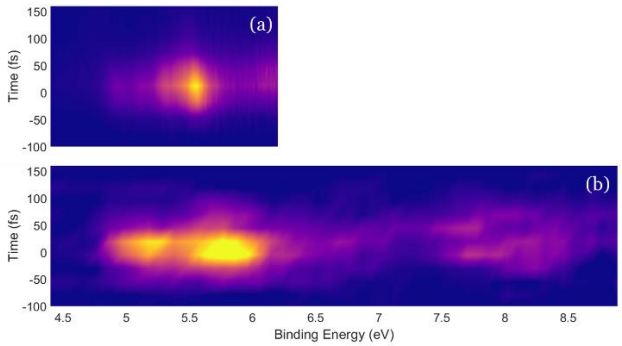

Figure 2. Time-resolved photoelectron spectra obtained following 268 nm excitation and ionization with two 400 nm photons corresponding to 6 eV (a) and with a 22.6 eV (b) photon.

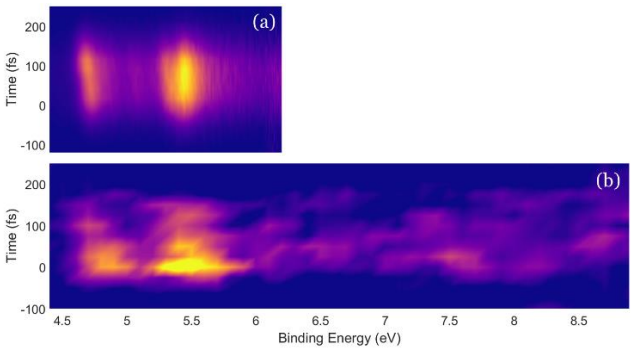

Figure 3. Time-resolved photoelectron spectra obtained following 254 nm excitation and ionization with two 400 nm photons corresponding to 6 eV (a) and with a 22.6 eV (b) photon.

between 4.8-6 eV. This broad feature contains two components resulting from ionisation of the excited state population in to the two spin orbit states of the ground ion state. The onset of the broad photoelectron band is due to ionisation into the $\tilde{X}$-$^2E_{3/2}$, while the dominant peak at 5.6 eV is due to ionisation into the $\tilde{X}$-$^2E_{1/2}$ state. The signal across this broad feature shows a very short excited state lifetime with the signal decaying within 30 fs. In the XUV measurements we see signals that at the same binding energies corresponding to ionisation into the $\tilde{X}$-states but the early time signal also has a second component at a binding energy of around 8 eV due to ionization into the A-state of the ion. The signals initially associated with the $\tilde{X}$-state show the same time dependence as in the UV signal, but between the signal associated with ionisation into the $\tilde{X}$ and A states we measure photoelectron intensity at later times. The signal forms a continuum that starts at energies associated with the $\tilde{X}$-states at early times and shift to higher binding energies as a function of time. The changes to higher binding energy shifts effectively map the extending C-I bond length as a function of pump-probe delay as the molecule moves from a bound systems into the asymptotic dissociation products. The dynamics following excitation on the red edge therefore follow what may be expected based on previous measurements and show rapid and direct dissociation with the photoelectron spectrum providing a sensitive measure of the changing geometric structure during the dissociation process.

Figure 3 presents the time-resolved spectra obtained with a pump energy around 254 nm, which is to the blue of the Q-band absorption maximum. On the blue side of the absorption maximum population can be transferred into the $^1Q_1$ and $^3Q_0$ states. At 254 nm we estimate between 10-20% of the total population is initially transferred into the $^1Q_1$ state with the remainder of the population in the $^3Q_0$ state as at 268 nm. In figure 3 a, we plot the data from the VMI experiments where the effective probe energy is 6 eV from two photon absorption of the 400 nm probe. Figure 3b is then the part of the XUV probe photoelectron spectrum, showing the excited state contribution to the overall signal. A quick visual comparison of the signals from the two pump wavelengths in figures 2 and 3 shows that the difference in signal between the two pump energies is striking. The higher energy pump photon leads to an extended lifetime of over 100 fs, with much more complex time dependent changes in the spectrum.

The early time spectrum measured at 254 nm shares many similarities to the 268 nm spectrum. At energies between 4.5-6 eV we see photoelectron bands associated with ionisation into the $\tilde{X}$ states. The distribution in intensity is now much more even but is still dominated by the signal into the $\tilde{X}$-$^2E_{1/2}$ state measured at around 5.4 eV. The second early time band at 8 eV is also present and corresponds to ionisation into the A-state of the ion. Focusing on the UV data in figure 3a) initially we see that as the delay between pump and probe is increased the intensity remains significant for over 100 fs and we see the intensity of the photoelectron bands move toward lower binding energies. This can also be seen (albeit more noisily) in the XUV probe spectrum in figure 3b). At the same time as this shift to lower binding energy we can also see shifts of the features associated with the $\tilde{X}$ band to higher binding energy, exactly as in the spectrum from the lower pump energy in figure 2b). The intensity initially associated with ionisation into the $\tilde{X}$-state therefore shifts to both lower and higher binding energies. The shifts in the photoelectron bands to higher binding energy occur on a very similar timescale to those observed at the 268 nm pump wavelength. These features are therefore most likely due to the same rapid C-I bond dissociation along the $^3Q_0$ potential. Other parts of the initial signal remain for a much longer lifetime, ~100 fs at 254 nm as opposed to ~30 fs at 268 nm, and shifts to lower binding energies before they decay in intensity and shift towards higher binding energies at later times. We suggest that this could be due to population on the $^1Q_1$ state that undergoes more complex dynamics before dissociation. These dynamics lead to a small but significant change in the Franck-Condon factors which leads to better overlap with lower vibrational states in the ion, effectively lowering the binding energy measured. Following this rearrangement the molecule redistributes its vibrational energy and dissociates over a much longer timescale.

The nature of the changing structure is however difficult to assign. In order to fully analyse these signals, careful calculation of the excited and ion state potential energy surfaces, accurate quantum dynamics simulations and calculation of the geometry dependent photoelectron spectrum are required. Each of these steps remain a real challenge to theory, with modern potential energy surface calculations still unable to match the absorption spectrum accurately.

Summary

In summary, we have performed a detailed experimental study of the photodissociation dynamics of methyl iodide across the red and blue edges of the Q-band absorption. The measured photoelectron spectra show that direct dissociation along the $^3Q_0$ potential dominates the dynamics on both edges, whereas the blue edge exhibits more complex dynamics originating from structural changes on the $^1Q_1$ state preceding dissociation, thus leading to much more complex spectra. A more detailed discussion of the UV probe VMI work is available in reference 12 and the details of the XUV probe will be the subject of a future manuscript.

Acknowledgements

R. S. M. thanks the Royal Society for a University Research Fellowship (UFUF150655). R. S. M. and J. W. thank the EPSRC for funding (EP/R010609/1). B. D. W. thanks the Central Laser Facility and Chemistry at the University of Southampton for a studentship. E. W. thanks Chemistry at the University of

Southampton for a studentship. A. K. acknowledges support from a Royal Society of Edinburgh Sabbatical Fellowship (58507) and a research grant from the Carnegie Trust for the Universities of Scotland (CRG050414). D. B. acknowledges an EPSRC studentship from the University of Edinburgh. We also acknowledge funding from the EC's Seventh Framework Programme (LASERLABEUROPE, grant agreement 228334). We thank John Dyke for very useful conversations and Phil Rice for technical assistance.

References

1. R. De Nalda, J. G. Izquierdo, J. Durá and L. Bañares, J. Chem. Phys., 2007, **126**, 021101.
2. M. E. Corrales, V. Loriot, G. Balerdi, J. González-Vázquez, R. De Nalda, L. Bañares and A. H. Zewail, Phys. Chem. Chem Phys., 2014, **16**, 8812–8818.
3. A. R. Attar, A. Bhattacherjee and S. R. Leone, J. Phys. Chem. Lett., 2015, **6**, 5072–5077.
4. F. Allum, M. Burt, K. Amini, R. Boll, H. Köckert, P. K. Olshin, S. Bari, C. Bomme, F. Braußе, B. Cunha de Miranda, S. Düsterer, B. Erk, M. Géléoc, R. Geneaux, A. S. Gentleman, G. Goldsztejn, R. Guillemin, D. M. P. Holland, I. Ismail, P. Johnsson, L. Journel, J. Küpper, J. Lahl, J. W. L. Lee, S. Maclot, S. R. Mackenzie, B. Manschwetus, A. S. Mereshchenko, R. Mason, J. Palaudoux, M. N. Piancastelli, F. Penent, D. Rompotis, A. Rouzée, T. Ruchon, A. Rudenko, E. Savelyev, M. Simon, N. Schirmel, H. Stapelfeldt, S. Techert, O. Travnikova, S. Trippel, J. G. Underwood, C. Vallance, J. Wiese, F. Ziaee, M. Brouard, T. Marchenko and D. Rolles, J. Chem. Phys., 2018, **149**, 204313.
5. M. E. Corrales, J. González-Vázquez, R. de Nalda and L. Bañares, J. Phy. Chem. Lett., 2019, **10**, 138–143.
6. A. Gedanken and M. D. Rowe, Chem. Phys. Lett., 1975, **34**, 39– 43.
7. A. D. Smith, E. M. Warne, D. Bellshaw, D. A. Horke, M. Tudorovskya, E. Springate, A. J. H. Jones, C. Cacho, R. T. Chapman, A. Kirrander and R. S. Minns, Phys. Rev. Lett., 2018, **120**, 183003.
8. F. Frassetto C. Cacho, C. A. Froud, I.C. E. Turcu, P. Villoresi, W. A. Bryan, E. Springate, and L. Poletto. Single-grating monochromator for extreme-ultraviolet ultrashort pulses. Opt. Express. 2011, **19**, 19169–19181.
9. A. D. Smith, H. M. Watts, E. Jager, D. A. Horke, E. Springate, O. Alexander, C. Cacho, R. T. Chapman and R. S. Minns, Phys. Chem. Chem. Phys., 2016, **18**, 28150–28156.
10. D. Bellshaw, D. A.Horke, A. D.Smith, H. M.Watts, E. Jager, E. Springate, O.Alexander, C. Cacho, R. T. Chapman, A. Kirrander and R. S.Minns. Ab-initio surface hopping and multiphoton ionisation study of the photodissociation dynamics of CS_2. Chem. Phys. Lett. 2017, **683**, 383–388.
11. D. A. Horke, H. M. Watts, A. D. Smith, E. Jager, E. Springate, O. Alexander, C. Cacho, R. T. Chapman, and R. S. Minns. Phys. Rev. Lett. 2016, **117**, 163002
12. E. M. Warne, B. Downes-Ward, J. Woodhouse, M. A. Parkes, D. Bellshaw, E. Springate, P. Majchrzak, Y. Zhang, G. Karras, A. S. Wyatt, R. T. Chapman, A. Kirrander and R. S. Minns. Phys. Chem. Chem. Phys. 2019, **21**, 11142-11149.